J-Researchers

Journal of Civil Engineering Researchers

Journal homepage: www.journals-researchers.com

Numerical Investigation of a Steel Frame Braced with a Central-Cylinder Cable System Using Shape Memory Alloy

MohammadReza Oliaei,[a,*] MohammadHadi Moallemi [a]

[a] *Department of Civil Engineering, Ramsar Branch, Islamic Azad University, Ramsar, Iran*

ABSTRACT

Conventional steel braces increase the risk of structural damage during earthquakes due to compressive buckling. In this study, the performance of a steel frame equipped with a memory alloy cable brace with a central cylinder is investigated through numerical modeling in ABAQUS. This system is expected to exhibit superior seismic performance compared to traditional braces due to characteristics such as superelasticity, self-centering, and energy dissipation, and to return to its initial state after an earthquake. It can significantly enhance the seismic performance of steel frames with minimal construction interference and reduced construction time. After model validation, this study evaluates the effects of cable type, memory alloy properties, and cable diameter on the lateral performance of the steel frame with central cylinder cable braces. The results indicate that even using steel cables in this system significantly increases strength, stiffness, and energy absorption compared to a frame without braces, although ductility decreases by 25%. Replacing the steel cable with a memory alloy cable simultaneously improves strength, stiffness, energy absorption, and ductility (by 10%) compared to the steel-cable specimen, compensating for the ductility reduction. Furthermore, enhancing the superelastic properties of the memory alloy increases the load-bearing capacity and absorbed energy, while increasing the memory alloy cable diameter (from 6 to 16 mm) improves all performance indicators, especially stiffness and strength, without significant loss of ductility. Overall, the results demonstrate that using memory alloy cables, along with optimizing their properties and diameter, is an effective approach for simultaneously improving strength, stiffness, ductility, energy dissipation, and seismic behavior of structures.

ARTICLE INFO

Received: November 09, 2025
Accepted: November 25, 2025

Keywords:
Numerical Development
Braced Steel Frame
Cable Brace System
Memory Alloy
ABAQUS

DOI: 10.61186/JCER.7.4.12
DOR: 20.1001.1.22516530.1399.11.4.1.1

1. Introduction

In lateral-resistant structures, permanent deformations caused by earthquakes reduce ductility and increase repair costs [1]; conventional strengthening methods also face drift and high acceleration limitations [2]. Experiments show that ordinary steel braces buckle during earthquakes, increasing the risk of collapse [3]; the Kobe earthquake investigation indicated that parts of structures collapsed or were severely damaged, highlighting the need to develop damage-reducing and self-centering systems [4]. Despite

* Corresponding author. Tel.: +989113924331; e-mail: m.r.oliaei@gmail.com.

higher construction costs, self-centering systems reduce life-cycle costs and improve seismic stability [5].

To enhance the lateral performance of braces, the use of high-strength steel cables has been proposed. These cables are lightweight, strong, and elastic, returning to their initial state after an earthquake, but they function only as tensile members [6]. Cable bracing systems absorb energy more effectively than traditional braces and improve stability [7]. Only-tension bracing systems and modern cable–cylinder systems have been introduced to overcome limitations, although low ductility remains a challenge [8][9]. The use of prestressed and post-tensioned cables combined with a central spring cylinder helps control lateral displacement, improve ductility, reduce seismic damage, and minimize the need for additional structural reinforcement [10]. This system is an improved version of the moment-resisting frame bracing, in which steel cables and pre-compressed springs reach ultimate strength under large displacements while remaining within the elastic range. This design reduces initial lateral stiffness and strength but increases stiffness during structural recovery, achieving more effective performance compared to ordinary braces [6].

Shape memory alloys (SMAs), with superelastic and self-recovering properties, are suitable for self-centering systems. SMA cables can recover large strains (up to 6–8%) without external stimuli and, with high energy dissipation, reduce drift and seismic response. By absorbing seismic energy and returning to their original shape, they decrease structural damage and repair requirements in braced frames [11][12].

This study investigates a steel frame with only-tension cross-cable bracing and a central spring cylinder, including a sample of SMA cable, under lateral loading using three-dimensional modeling in ABAQUS [13]. Validation is performed using the experimental results of Mehrabi et al. [14]. The effects of cable material type (steel and SMA) and cable diameter on the lateral behavior of the structure—including strength, stiffness, ductility, lateral energy dissipation, and deformations—are evaluated through numerical analysis and parametric studies. Results are presented and compared using load–displacement curves and analytical tables to propose a novel approach for improving the seismic performance of frames.

2. Validation of the Model Simulation Process

The modeling and seismic analysis of structures, particularly using the finite element method (FEM), have advanced significantly in recent decades. This approach, utilizing software such as ANSYS and ABAQUS, enables detailed and complex analyses of structural systems. Today, ABAQUS is recognized as a critical tool for nonlinear structural analysis and engineering design.

The present study investigates the damage in steel frames braced with tension cables through nonlinear quasi-static analysis using ABAQUS, and compares the results with various experimental tests. This highlights the importance of calibrating analytical software to ensure the accuracy of both modeling and results in nonlinear analyses.

To evaluate the accuracy of finite element modeling in this study, three steel frames braced with tension cables, previously tested by Mehrabi et al. [14], were selected. The experiments (as shown in Figure 1) included three laboratory specimens (each with a column length of 1595 mm and a beam length of 1275 mm): an unbraced steel frame (BF), a cable-cross-braced steel frame without cable

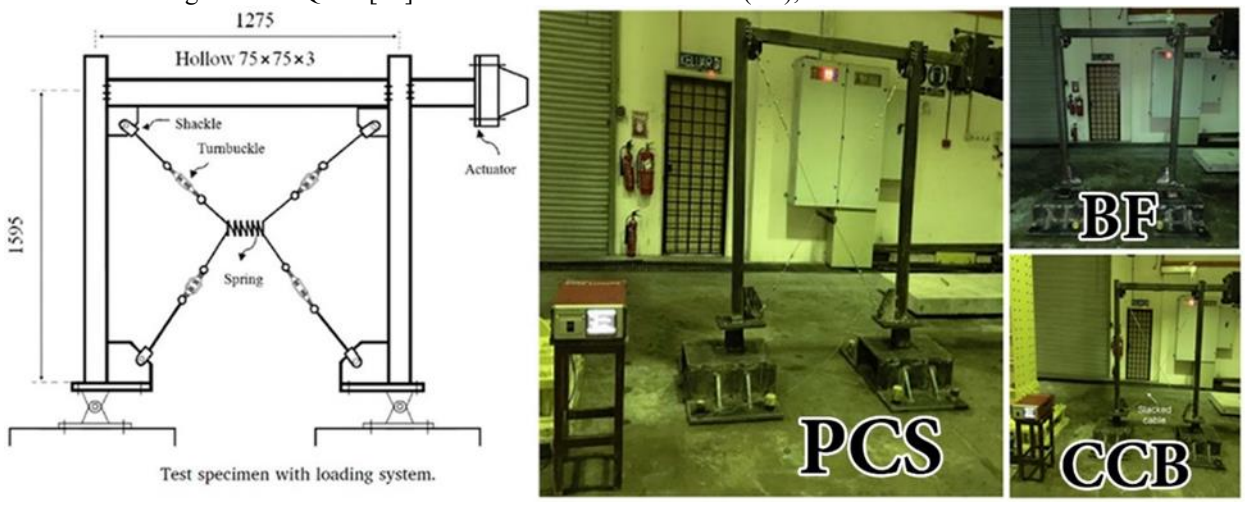

Figure 1 – Image of the three laboratory specimens and dimensional details of the cable- and spring-braced moment frame studied by Mehrabi et al. [14] under lateral cyclic loading.

connections at the frame center (CCB), and a cable-cross-braced steel frame with a spring connection at the frame center (PCS). The cable bracing system used steel cables with a nominal diameter of 6 mm and a full prestress corresponding to approximately 2% lateral column displacement. The steel frames had pinned supports, with beam and column sections measuring 75 × 75 mm, flange thickness 3 mm, and web thickness 2 mm.

The specimens were subjected to lateral cyclic loading, and their experimental results—based on material properties (including steel, cable, and spring) listed in Table 1—were obtained in the lateral load–displacement hysteresis curves (Figure 2). Subsequently, numerical modeling was performed using ABAQUS (Figure 2), and the results were compared with experimental data.

For load application and boundary conditions at the lower support, a reference point with a coupling constraint was created at the top of the specimen using ABAQUS Interaction module. Additionally, as shown in Figure 2, for the CCB and PCS specimens, the interaction between the steel plate and the cable required four Tie constraints with full fixation. In the PCS specimen, due to the presence of the spring system, surface contact was defined with a friction coefficient of 0.30 between the steel, cable, and spring.

In the numerical simulation, increasing mesh density improves accuracy but also increases computation time, so a balance must be maintained. To reduce computational costs, quasi-static analysis was conducted using C3D8R elements for springs and S4R elements for the steel frame.

Comparison of the load–displacement curves of the specimens (Figure 2) with experimental and numerical results showed that the numerical model adequately simulated the behavior of the specimens, confirming model validation. Moreover, finite element analysis results indicate that the maximum shear forces for the experimental specimens and the finite element models are nearly identical, with only a 5.7% difference in peak values.

Table 1
Material properties (steel, cable, and spring) used in the three laboratory specimens [14].

Mechanical Properties of Steel in Frame

Type	Steel Grade	Yield Strength (MPa)	Ultimate Strength (MPa)	Elastic Modulus (GPa)	Density (kg/m³)
Column	A36	360	420	205	7800
Beam	A36	360	420	205	7800

Mechanical Properties of Wire Rope Unit

Type	Dia. (mm)	Yield Strength (MPa)	Yield Strain	Tensile Strength (MPa)	Elastic Modulus (GPa)	L (mm)	W (mm)
Wire Rope	6	1016	0.01	1765	123.5	–	–
Hook and Eye Turnbuckle	8	305	0.004	515	205	–	–
DEE Shackles	10	305	0.004	515	205	25	13

Material Properties of Spring

Material	Spring Length (mm)	Spring Diameter (mm)	Elastic Modulus (GPa)	Modulus of Rigidity (GPa)	Density (kg/m³)
Stainless Steel	100	40	193	69	7920

3. Analysis of Findings

In this study, after validating the laboratory results (with good agreement), the effects of various parameters such as cable type, properties of the shape memory alloy (SMA) material, and cable diameter on lateral performance are evaluated. In this section, to extend the numerical work of Kherabi et al. [14], cyclic load–displacement hysteresis diagrams will be used to illustrate lateral performance, and metrics such as strength, stiffness, ductility, and lateral energy dissipation will be calculated and compared to assess the structural lateral behavior. Therefore, this section includes the following:

- Evaluation and comparison of the lateral performance of steel frames
- Effect of using SMA cables on the lateral performance of the cable-braced frame system with a central cylinder instead of steel cables
- Effect of changing the superelastic properties of SMA cables on the lateral performance of the cable-braced frame system with a central cylinder
- Effect of changing the diameter of SMA cables on the lateral performance of the cable-braced frame system with a central spring cylinder

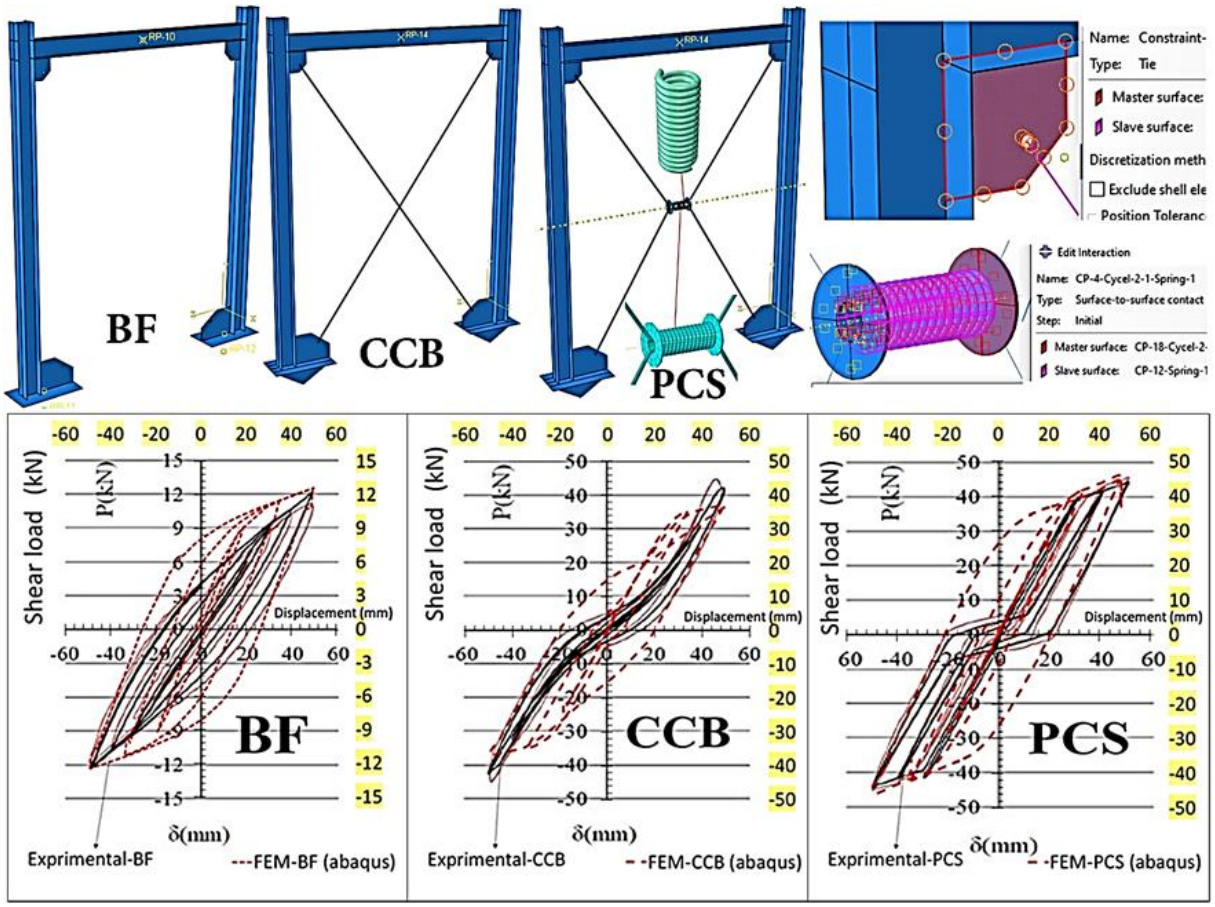

Figure 2 – Numerical modeling and validation for the three laboratory specimens [14] of the cable-braced moment frame.

3.1. Lateral Performance of Steel Frames under Study

In this part of the research, since a reference specimen is required to compare the other parametric samples against, the lateral performance of the reference specimens is examined. Two frames were selected as reference specimens: a bare frame (denoted as "BF") and a cable-braced frame with a central cylinder (denoted as "RF"). Figure 3 shows the comparison of their hysteresis diagrams.

As shown in Figure 3, the load–displacement hysteresis diagrams of BF and RF indicate how these specimens respond to lateral cyclic loading. Additionally, Figure 3 presents the envelope of the hysteresis and its bilinear approximation, where the envelope is obtained from the maximum resistances corresponding to each cyclic displacement. The bilinear diagram uses the equivalent energy method to convert the multi-linear envelope into a simpler form so that the areas under both diagrams are equal, ensuring that the absorbed energy remains the same. In this diagram, the failure point is recognized as the yield point; for the positive and negative directions, the effective ultimate displacement is denoted by Δu, the displacement at the failure point by Δy, and the resistance at the failure point by Vy.

In the analysis of these specimens or similar systems, the lateral load–displacement diagram serves as the basis for evaluating lateral performance, where:

- Maximum lateral resistance (P) represents the frame strength
- Initial stiffness (K), obtained by dividing the yield resistance by the yield displacement (Vy/Δy)
- Ductility (μ), calculated as the ratio of effective ultimate displacement to yield displacement (Δu/Δy)
- Energy dissipation, computed from the area inside the hysteresis loops

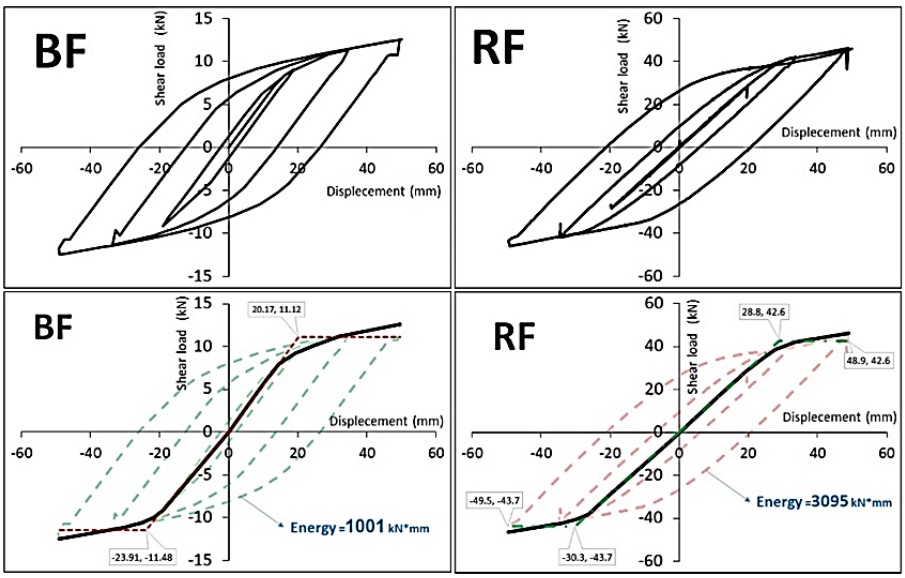

Figure 3. Comparison of load–displacement hysteresis diagrams of the two reference specimens: bare frame "BF" and cable-braced frame with a central cylinder "RF".

Table 2

Comparison of lateral performance: bare frame "BF" and cable-braced frame with a central cylinder "RF".

Spectrum	Energy (kN·mm)	P+ (Pos) kN	P- (Neg) kN	System Hardness K+ (Pos) kN/m	K- (Neg) kN/m	μ+ (Pos) kN/m	μ- (Neg) kN/m
RF	3095	46.2	46.4	1481	1444.5	1.7	1.64
BF	1001	12.6	12.5	551.4	480.19	2.45	2.05
	209%	267%	272%	169%	201%	-31%	-20%

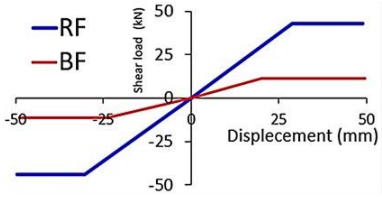

This energy-based approach, aided by finite element software, allows precise determination of performance parameters and provides a suitable basis for pushover analysis and retrofit design.

To determine the energy dissipation of the bare frame and the steel frame braced with a cable system, the area inside the load–displacement hysteresis loops must be calculated, which can be done using Excel by analyzing numerical data. According to Table 2, the results show that using a steel cable-braced frame system with a central cylinder, compared to a bare frame, significantly improves lateral performance, with an average increase of 209% in energy dissipation, 270% in strength, and 185% in stiffness, while ductility decreases by 25%.

Based on Table 2, the improved performance of the RF specimen can be attributed to the increase in displacement and yield resistance. By providing lateral bracing with crossed steel cables along with a central cylinder, the frame exhibits higher displacement and resistance at yielding, which increases the resistance, stiffness, and energy dissipation of the RF specimen.

3.2. Effect of Using SMA Cables on Lateral Performance

This section of the study investigates how the lateral performance of a steel frame equipped with a cable bracing system changes if memory alloy (SMA) cables are used instead of steel cables. Additionally, it examines the difference in lateral performance compared to a steel frame with a central-cylinder steel cable bracing system. To this end, it is first necessary to have a good understanding of the SMA material intended for the cables. Accordingly, the superelastic and reversible behavior of the SMA materials used in this study is explained below:

In recent years, SMAs have attracted significant attention in civil engineering due to their excellent

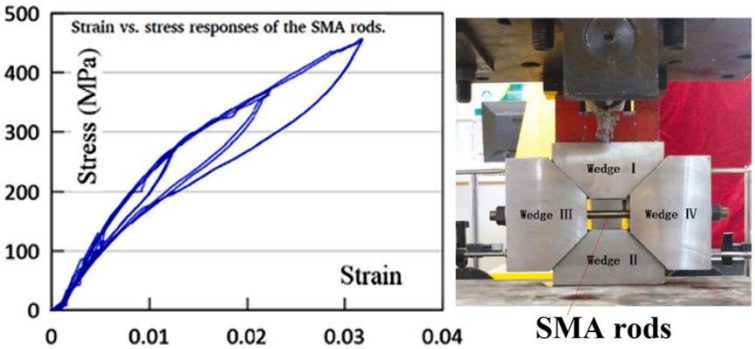

Figure 4 – Sample and stress-strain diagram of the superelastic SMA rod studied by Zhang et al. [11].

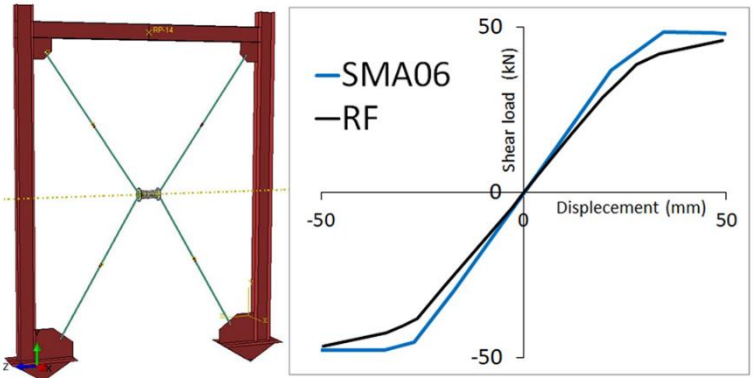

Figure 5 – Numerical model of the steel frame with SMA cable bracing system and comparison with the steel cable frame

superelastic capabilities and moderate energy dissipation. Derivatives of these materials have been considered for self-centering systems because of the inherent nonlinear elastic behavior of SMAs [15]. SMAs are metallic alloys that can recover their original shape after deformation due to a solid-to-solid phase transformation. Superelastic SMAs can recover large deformations after unloading without any external stimulus [15].

The stress-strain diagram of these materials (as shown in Figure 4) exhibits a "flag-shaped" form in tension and compression, with two stages or phases. The initial linear behavior, like other materials, has a defined elastic modulus and Poisson's ratio [16]. In Abaqus software (version 2019 onward), superelastic material properties are included. According to this, the martensite Young's modulus (EM) and martensite Poisson's ratio (νM) in the second tensile phase must be defined. Key input parameters for defining superelastic materials include: strain range between the Young's modulus and martensite modulus (εL), initial and final stress of loading and unloading in tension, initial stress of loading in compression, reference temperature, and loading parameters. The final plastic strain of the SMA material can also be defined in its settings.

The stress-strain curve of the superelastic SMA rod tested in the lab was taken from a centrally damped specimen with SMA rods under lateral loading, studied by Zhang et al. [16], as shown in Figure 4. The material properties of the SMA were recorded in the numerical model based on this data.

Numerical loading (as shown in Figure 5) was applied to the steel frame equipped with the SMA cable bracing system, designated as "SMA06." This designation refers to the sample being modeled and analyzed with 6 mm diameter SMA cables. Figure 5 shows the hysteresis load-displacement curve of the "SMA06" specimen compared with the corresponding curve of the reference steel cable bracing frame, "RF," indicating that the "SMA06" specimen exhibits higher performance.

According to the hysteresis loading results on the "SMA06" specimen, the hysteresis loop area, representing the system's energy dissipation, is calculated as 3553 kN·mm. By evaluating lateral performance indices such as strength, stiffness, ductility, and energy dissipation, the lateral performance of the SMA-braced steel frame can be quantified. Table 3 presents these performance metrics alongside the reference steel cable frame (RF).

From Table 3, it can be inferred that implementing an SMA central-cylinder cable bracing system improves the lateral performance of the steel frame compared to the steel cable bracing system. This improvement includes increases in system strength, stiffness, ductility, and energy dissipation, with lateral energy dissipation increasing by 15%, mean lateral strength by 4.5%, mean lateral stiffness by 18.5%, and mean lateral ductility by 10%. These

Table 3
Lateral performance of steel frames with SMA cable bracing and central-cylinder steel cable bracing systems.

		Reaction Force		System Hardness		Ductility	
Spectrum	Energy (kN*mm)	P+ (Pos) (kN)	P- (Neg) (kN)	K+ (Pos) (kN/m)	K- (Neg) (kN/m)	μ+ (Pos) (kN/m)	μ- (Neg) (kN/m)
RF	3095	46.2	46.4	1481	1444.5	1.7	1.64
SMA06	3553	48.8	47.9	1726	1727.3	1.83	1.83
	15%	6%	3%	17%	20%	8%	12%

Table 4
SMA samples considered for application in steel frames with central-cylinder cable bracing systems

Mechanical Property	E_A (GPa)	E_M (GPa)	σ_{StL} (MPa)	σ_{EtL} (MPa)	σ_{StU} (MPa)	σ_{EtU} (MPa)
SMA06	27	31	170	455	250	50
SMA06-01	54	62	340	910	500	100
SMA06-02	13.5	15.5	85	227.5	125	25

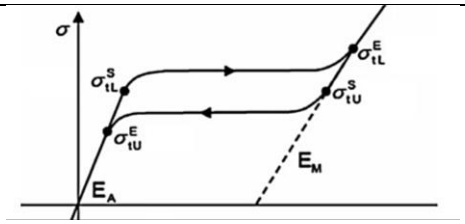

Table 5
Lateral performance of steel frames with central-cylinder SMA cable bracing and effect of modified SMA properties.

		Reaction Force		System Hardness		Ductility	
Spectrum	Energy (kN*mm)	P+ (Pos) (kN)	P- (Neg) (kN)	K+ (Pos) (kN/m)	K- (Neg) (kN/m)	μ+ (Pos) (kN/m)	μ- (Neg) (kN/m)
RF	3095	46.2	46.4	1481	1444.5	1.7	1.64
SMA06	3553	48.8	47.9	1726	1727.3	1.83	1.83
SMA06-01	3878	52.6	56.6	1793	1825.1	1.75	1.6
SMA06-02	3432	45.4	44.5	1587	1618.5	1.77	1.81

changes highlight the advantages of using SMAs to enhance the performance of braced structures.

3.3. Effect of Changing SMA Cable Superelastic Properties on Lateral Performance

This section examines how changes in the SMA material properties assigned to the steel cable bracing system affect the lateral performance of the steel frame. Additionally, it evaluates the differences in lateral performance compared to the central-cylinder steel cable bracing frame. Several factors are considered for modifying SMA properties, as shown in Table 4.

As seen in Table 4, SMA samples are introduced for use in steel frames with central-cylinder cable bracing. The first sample, “SMA06,” is the default SMA whose lateral performance was detailed in the previous section. The “SMA06-01” and “SMA06-02” samples differ from the default SMA06. By examining the table, it can be observed that the properties of SMA06-01 are twice those of the default SMA06, while SMA06-02 properties are half.

These properties include two elastic moduli (EA and EM) for the two linear behaviors of the superelastic material. σStL and σEtL correspond to the start and end stresses of linear deformation during loading, while σStU and σEtU correspond to the start and end stresses during unloading. The modified SMA materials must be assigned in a separate file to replace the default SMA cables.

To determine the energy dissipated by the steel frame with the modified SMA cables, the area inside all new hysteresis load-displacement curves must be calculated. The energy dissipation of the double-property SMA sample is 3887 kN·mm, and that of the half-property SMA sample is 3432 kN·mm. By evaluating lateral performance indices such as strength, stiffness, ductility, and energy dissipation, the lateral performance of the steel frame with modified SMA cables can be quantified. Table 5 presents these values alongside the reference frame.

From Table 5, it can be concluded that doubling the elastic properties of the SMA cable increases energy dissipation, lateral strength, and stiffness by 9.1%, 7.9%, and 3.9%, respectively, but reduces ductility by 4.7%.

Conversely, halving the SMA elastic properties decreases energy dissipation, strength, and stiffness by 3.4%, 13.7%, and 11.5%, respectively, while ductility increases by 1.5%.

3.4. Effect of SMA Cable Diameter on Lateral Performance

This section of the study addresses the question of how the lateral performance of a steel frame equipped with a central-cylinder cable bracing system changes if the diameter of the cable modeled with a shape memory alloy (SMA) is altered. In this context, three cable diameter scenarios were considered. The existing cable diameter is 6 mm, and the two new diameters to be evaluated are 10 mm and 16 mm. The new specimens for these two diameters are labeled "SMA10" and "SMA16," respectively.

Numerical loading (as shown in Figure 5) was applied to the steel frame specimens "SMA10" and "SMA16," and their hysteresis loading results were obtained. To determine the energy absorbed by the steel frame equipped with the central-cylinder cable bracing system with the new SMA, the area of the loops within the hysteresis load–displacement diagram was calculated. This represents the energy absorption for cable diameters of 10 and 16 mm, which were found to be 3585 and 3612 kN·mm, respectively. By evaluating the lateral performance criteria—strength, stiffness, ductility, and energy absorption—of the SMA cable-braced steel frame specimens, the lateral performance levels can be quantified. Table 6 presents these performance measures alongside the reference steel frame (steel frame braced with a central-cylinder steel cable system).

From the results in Table 6, it can be inferred that implementing a central-cylinder cable bracing system with SMA cables of 10 and 16 mm diameter improves the lateral performance of the steel frame compared to the lateral performance of the reference steel frame with a central-cylinder steel cable bracing system. The results indicate that increasing the SMA cable diameter from 6 mm to 10 mm and finally to 16 mm increases the lateral energy absorption by 14.8%, 15.8%, and 16.7%, respectively, compared to the reference steel cable frame. Similarly, the lateral ductility increases by 10%, 5%, and 5.2%, respectively. The lateral strength increases by 4.3%, 9.8%, and 19.3%, and the lateral stiffness increases by 18.1%, 23.9%, and 34.6% with the same diameter increments.

4. Overall Comparison of Results

In this part of the study, the lateral performance data obtained for the central-cylinder steel cable-braced frame and the various scenarios are compiled to evaluate their overall behavior under lateral loading. Table 7 summarizes all the specimens considered in this study.

Table 6
Lateral performance of SMA cable specimens with diameters of 10 and 16 mm for use in steel frames braced with a central-cylinder cable system

		Reaction Force		System Hardness		Ductility	
Spectrum	Energy (kN*mm)	P+ (Pos) (kN)	P- (Neg) (kN)	K+ (Pos) (kN/m)	K- (Neg) (kN/m)	μ+ (Pos) (kN/m)	μ- (Neg) (kN/m)
RF	3095	46.2	46.4	1481	1444.5	1.7	1.64
SMA06	3553	48.8	47.9	1726	1727.3	1.83	1.83
SMA10	3330	51.3	50.5	1783	1841	1.8	1.7
SMA16	3587	55.8	54.8	1956	1980.4	1.83	1.68

Table 7
Comprehensive table of all studied specimens, central-cylinder cable-braced steel frames under lateral loading.

		Reaction Force		System Hardness		Ductility	
Spectrum	Energy (kN*mm)	P+ (Pos) (kN)	P- (Neg) (kN)	K+ (Pos) (kN/m)	K- (Neg) (kN/m)	μ+ (Pos) (kN/m)	μ- (Neg) (kN/m)
RF	3095	46.2	46.4	1481	1444.5	1.7	1.64
SMA06	3553	48.8	47.9	1726	1727.3	1.83	1.83
SMA06-01	3878	52.6	56.6	1793	1825.1	1.75	1.6
SMA06-02	3432	45.4	44.5	1587	1618.5	1.77	1.81
SMA10	3330	51.3	50.5	1783	1841	1.8	1.7
SMA16	3587	55.8	54.8	1956	1980.4	1.83	1.68

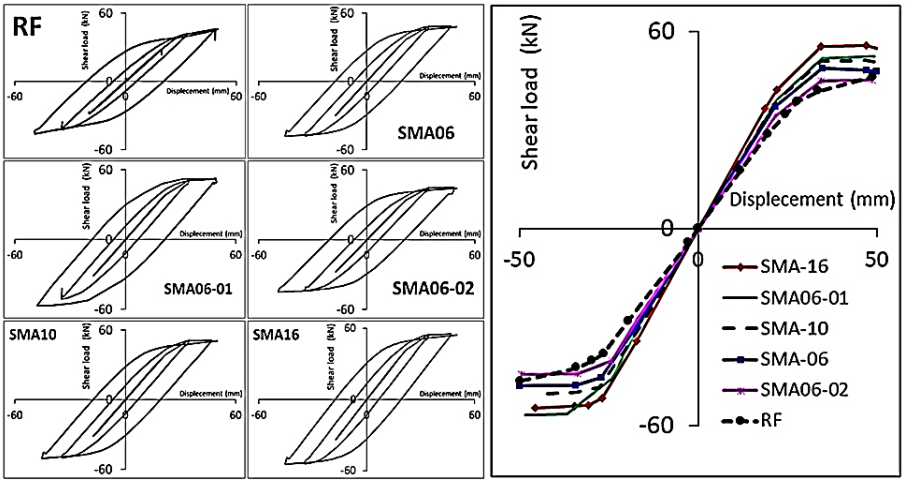

Figure 5. Hysteresis load–displacement and lateral envelope curves for all numerical specimens under study.

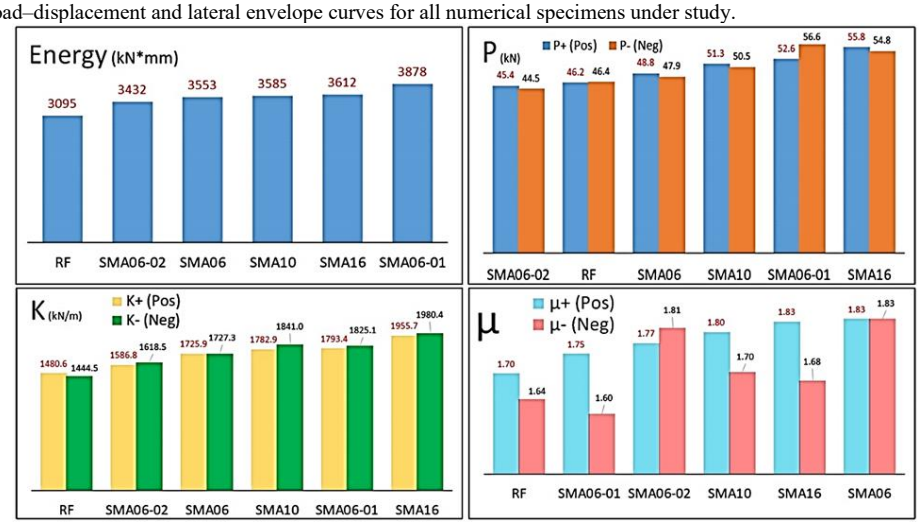

Figure 6 – Lateral energy absorption, strength, stiffness, and ductility of all numerical specimens under study.

According to Table 7, the four seismic performance criteria—energy absorption, strength, stiffness, and lateral ductility—can be compared across the six central-cylinder steel cable-braced frame configurations. Figures 5 and 6 illustrate the hysteresis and envelope curves, as well as the lateral energy absorption, strength, stiffness, and ductility for all numerical specimens considered.

Based on Figures 5 and 6, the following observations can be made regarding the hysteresis and envelope curves, as well as energy absorption, strength, stiffness, and ductility of all specimens:

- The comparison of lateral performance in cyclic loading shows that the main criteria—energy absorption, strength, stiffness, and ductility—were evaluated for six different cases, and the related plots illustrate the differences and advantages of each system.
- The results indicate that the SMA cable-braced steel frame specimen with double elastic properties ("SMA06-01") exhibited the highest lateral energy absorption, followed by the specimens with cable diameters of 16 mm, 10 mm, and 6 mm ("SMA16," "SMA10," and "SMA06," respectively). Even the specimen with half the initial elastic properties ("SMA06-02") performed better in energy absorption than the reference steel cable frame.
- In terms of lateral strength, the SMA cable-braced specimen with 16 mm diameter ("SMA16") had the highest value, followed by "SMA06-01," "SMA10," and "SMA06," while "SMA06-02" showed lower strength than the reference steel cable-braced frame.
- The SMA 16 mm specimen ("SMA16") also exhibited the highest lateral stiffness, followed by "SMA06-01," "SMA10," and "SMA06," with "SMA06-02" still outperforming the reference steel cable frame in stiffness.
- Regarding ductility, the 6 mm SMA cable frame ("SMA06") had the highest lateral ductility,

followed by 16 mm and 10 mm SMA specimens ("SMA16" and "SMA10"), while the reference steel cable frame had the lowest.

5. Conclusion

Considering the importance of improving the seismic performance of steel structures, this study evaluated the effects of cable type, SMA properties, and cable diameter on steel frames equipped with central-cylinder cable bracing systems. The goal was to investigate changes in strength, stiffness, ductility, and lateral energy absorption under different scenarios and to propose effective strategies for enhancing seismic behavior. The research methodology was based on numerical simulations and comparison with baseline data, with performance metrics extracted from hysteresis load–displacement and bilinear envelope curves. The main findings are as follows:

- Using the system, even with steel cables, increased strength, stiffness, and energy absorption by 270%, 185%, and 209%, respectively, compared to the unbraced frame, although ductility decreased by 25%. Replacing steel cables with SMA simultaneously increased strength (4.5%), stiffness (18.5%), energy absorption (15%), and ductility (10%), compensating for the ductility reduction.
- Doubling the superelastic properties of SMA increased load capacity and energy absorption but slightly decreased ductility; halving these properties had the opposite effect. Increasing the SMA cable diameter from 6 to 10 and 16 mm improved all indices, especially stiffness (up to 34.6%) and strength (up to 19.3%), without noticeable ductility loss.
- Load–displacement curves showed that the SMA cable with double properties and 6 mm diameter ("SMA06-01") had the highest energy absorption, while the 16 mm cable specimen ("SMA16") exhibited the greatest strength and stiffness. Even the half-property specimen ("SMA06-02") outperformed the conventional steel system in stiffness and energy absorption. In ductility, the 6 mm SMA cable performed best, and the conventional steel system performed worst.
- The central-cylinder cable bracing system, even with steel cables, significantly increases strength, stiffness, and energy absorption, but reduces ductility. Using SMA cables instead of steel simultaneously enhances strength, stiffness, energy absorption, and ductility, offsetting ductility loss.
- Enhancing SMA elastic properties improves strength and energy absorption but slightly reduces ductility; decreasing these properties has the opposite effect. Increasing SMA cable diameter is an effective way to improve all lateral performance indicators, especially stiffness and strength.

In summary, the results demonstrate that using SMA cables in central-cylinder cable bracing systems, along with optimization of properties and cable diameter, is an efficient approach to increase strength, stiffness, ductility, and energy absorption and to improve seismic performance.

References

[1] Hu, X., J.-W. Bai, K. Khandelwal, and M. Bruneau. "Mitigation of residual deformations in eccentrically braced frames through a low-cost re-centering mechanism." Earthquake Engineering & Structural Dynamics 50.14 (2021): 3660–3678. https://doi.org/10.1002/eqe.4113

[2] Lavan, O. "Seismic design and retrofit procedure for total accelerations and inter-story drifts reduction of buildings with protective systems." In Proceedings of the 9th U.S. National and 10th Canadian Conference on Earthquake Engineering (Paper No. 359). Toronto, Canada (2010).

[3] Issa, A., S. Stephen, and A. Mwafy. "Unveiling the seismic performance of concentrically braced steel frames: A comprehensive review." Sustainability 16.1 (2024): 427. https://doi.org/10.3390/su16010427

[4] Sakellariadis, L., I. Anastasopoulos, and G. Gazetas. "Fukae bridge collapse (Kobe 1995) revisited: New insights." Soils and Foundations 60.6 (2020): 1450–1467. https://doi.org/10.1016/j.sandf.2020.09.005

[5] Hu, S., W. Wang, M. S. Alam, and K. Ke. "Life-cycle benefits estimation of self-centering building structures." Engineering Structures 284 (2023): 115982. https://doi.org/10.1016/j.engstruct.2023.115982

[6] Xu, G., T. Guo, and A. Li. "Development and investigation of a self-centering cable brace with variable slip stiffness for braced frame structure." Journal of Building Engineering 76 (2023): 107383. https://doi.org/10.1016/j.jobe.2023.107383

[7] Ghasemi, M., C. Zhang, H. Khorshidi, and L. Sun. "Seismic performance assessment of steel frames with slack cable bracing systems." Engineering Structures 250 (2022): 113437. https://doi.org/10.1016/j.engstruct.2021.113437

[8] Xu, G., T. Guo, A. Li, Y. Wu, H. Zhang, and G. Zhi. "Innovative self-centering tension-only braces for enhanced seismic resilience in frame structures: An experimental and numerical analysis." Engineering Structures 319 (2024): 118816. https://doi.org/10.1016/j.engstruct.2024.118816

[9] Fanaie, N., and E. Afsar Dizaj. "Cable-cylinder bracing system: Theoretical background, structural behavior, and seismic design coefficients." In Seismic Evaluation, Damage, and Mitigation in Structures, edited by I. Mansouri and P. O. Awoyera, 51–94. Woodhead Publishing (Elsevier) (2022). https://www.sciencedirect.com/book/9780323885317

[10] Chou, C.-C., and L.-Y. Huang. "Mechanics and validation tests of a post-tensioned self-centering brace with adjusted stiffness and

deformation capacities using disc springs." Thin-Walled Structures 195 (2024): 111430. https://doi.org/10.1016/j.tws.2024.111430

[11] Casagrande, L., C. Menna, D. Asprone, M. Ferraioli, and F. Auricchio. "Buildings." In Shape Memory Alloy Engineering (2nd ed.), 689–729. Elsevier (2021). https://doi.org/10.1016/B978-0-12-819264-1.00021-2

[12] Askariani, S. S., S. Garivani, I. Hajirasouliha, and N. Soleimanian. "Innovative self-centering systems using shape memory alloy bolts and energy dissipating devices." Journal of Constructional Steel Research 190 (2022): 107127. https://doi.org/10.1016/j.jcsr.2021.107127

[13] ABAQUS-V6.19-1. "Finite Element Analysis Software." Johnston, RI, USA. ABAQUS/Standard theory. Manual, Dassault Systèmes Simulia Corp. (2019).

[14] Mehrabi, M. H., Z. Ibrahim, S. S. Ghodsi, and M. Suhatril. "Seismic characteristics of X-cable braced frames bundled with a precompressed spring." Soil Dynamics and Earthquake Engineering 116 (2019): 732–746. https://doi.org/10.1016/j.soildyn.2018.10.014

[15] Lagoudas, D. C., and J. G. Boyd. "Shape memory alloys in civil engineering: Applications and challenges." Materials Science and Engineering: R: Reports 140 (2019): 1-22. https://doi.org/10.1016/j.mser.2019.01.001

[16] Zhang, S., et al. "Tests of a novel re-centering damper with SMA rods and friction wedges." Engineering Structures 236 (2021): 112125. https://doi.org/10.1016/j.engstruct.2021.112125